

# Realization of Low Frequency Oscillation Free Operation in a Hall Thruster

IEPC-2007-88

*Presented at the 30<sup>th</sup> International Electric Propulsion Conference, Florence, Italy  
September 17-20, 2007*

Taichiro TAMIDA<sup>\*</sup>, Ikuro SUGA<sup>†</sup>  
*Advanced Technology R&D Center, Mitsubishi Electric Corporation  
8-1-1 Tukaguchi-honmachi, Amagasaki, Hyogo, 661-8661, Japan*

Takafumi NAKAGAWA<sup>‡</sup>, Hiroyuki OSUGA<sup>§</sup>, Toshiyuki OZAKI<sup>\*\*</sup>  
*Space System Department, Kamakura Works, Mitsubishi Electric Corporation,  
325Kamimachiya, Kamakura, Kanagawa, 247-8520, Japan*

*and*

Katsuaki MATSUI<sup>††</sup>  
*Institute for Unmanned Space Experiment Free Flyer2-12  
Kanda-Ogawamachi, Chiyoda-Ku, Tokyo, 101-0052, Japan*

**Abstract:** We performed a theoretical and experimental study of low-frequency oscillation in a Hall thruster. The oscillation phenomenon depends on various external control parameters. However, we found that such dependence can be observed very clearly using certain expressions, which are combinations of external control parameters. Using these expressions, one can observe the oscillation strength and oscillation mode for a given set of external control parameters. We considered that low-frequency oscillation can be essentially suppressed by a method of determining parameter sets. This method would be especially important when the external control parameters are transiently changes. We show that, controlling the power conditioners synchronously, stable and oscillation-free thruster start-up can be realized using the method. The method of determining the parameter sets is very important for Hall thruster design and control; in particular, it makes it easy to manage electromagnetic compatibility with the other equipments in a satellite, using a power supply control.

---

<sup>\*</sup> Senior Researcher, Power electronics System Development Center, Tamida.Taichiro@aj.MitsubishiElectric.co.jp

<sup>†</sup> Manager, Power electronics System Development Center, Suga.Ikuro@ay.MitsubishiElectric.co.jp

<sup>‡</sup> Engineer, Space system Department, Nakagawa.Takafumi@dp.MitsubishiElectric.co.jp

<sup>§</sup> Senior engineer, Space system Department, Osuga.Hiroyuki@bx.MitsubishiElectric.co.jp

<sup>\*\*</sup> Senior engineer, Space system Department, Ozaki.Toshiyuki@dr.MitsubishiElectric.co.jp

<sup>††</sup> Senior Researcher, Advanced Satellite Project Department, matsui@usef.or.jp

## I. Introduction

An electric propulsion system is an essential technology for the orbit control of satellites in space. Considering recent requirements for satellites, such as a saving of the control time, a large thrust, and an optimal electric power distribution, we proceed with the development of Hall thrusters [1] with high thrust efficiencies. We also proceed with the development of a power-processing unit (PPU) for a Hall thruster [2], with the following objectives; to optimize a PPU design for a Hall thruster drive, to optimally control the Hall thruster using the PPU, and to autonomously control the entire Hall thruster system.

One of the most important problems for the practical applications of Hall thrusters is discharge current oscillation. Although a constant DC voltage is applied, the thrust or discharge current oscillates, particularly in the frequency range of 10 - 100 kHz (low-frequency oscillation) [3]. The suppression of current oscillation is an essential challenge to be solved for the practical applications of the thrusters, not only to determine the effects of such oscillation on the thruster operation, reliability, and lifetime, but also to control electromagnetic compatibility (EMC) with the other equipments installed in a satellite.

Many theoretical studies on low-frequency oscillation have been conducted [4][5], revealing that such oscillation is caused by ionization instability. However, there are no clear guidelines for a low-frequency-oscillation-free operation, and practical operation conditions are determined experimentally and empirically.

The objectives of this study are to clarify the conditions for a low-frequency-oscillation-free operation and realize a stable operation over a wide operating range of a Hall thruster [6]. By applying the guidelines described in this paper, we consider that low-frequency oscillation can be essentially suppressed and that many problems, such as that on the EMC, can be solved.

## II. Experimental Setup

Figure 1 shows the axial cross section of the Hall thruster, the block diagram of power supplies and the mass flow controller for propellant gas. The Hall thruster we developed is of a magnetic layer type [7], which is typified by a stationary plasma thruster (SPT).

The Hall thruster is equipped with power conditioners (PCs) for an anode electrode, an inner magnetic coil and outer magnetic coils. Xe gas is supplied through a mass flow controller (MFC). The currents of the inner and outer magnetic coils can be individually regulated. However, in this study, to simplify experimental conditions, the same current  $I_c$  is always applied to both coils.

A hollow cathode is fitted externally because the Hall thruster requires an external electron source. The PCs are fitted for a keeper electrode and a cathode heater electrode. The MFC is also used to supply Xe gas to the hollow cathode. As long as the hollow cathode operates stably, it rarely affects the oscillation phenomenon. Therefore, we did not consider the operation conditions of the hollow cathode in this study.

The operation conditions are determined by three parameters: the anode voltage  $V_a$ , propellant gas flux  $Q$ , and inner and outer magnetic coil currents  $I_c$ . The oscillation is detected by measuring the anode current  $I_a$ . Here,  $Q$  indicates the gas flux of the Hall thruster and does not include the gas flux of the hollow cathode.

## III. Measurement of Oscillating Waveforms

Figure 2 shows the measured typical oscillating anode current and voltage waveforms. The anode current waveform oscillates violently, and the anode voltage waveform fluctuates. One of the reasons for the voltage fluctuation is the capacity of the power supply that is not sufficiently large. Figure 3 shows the results of the

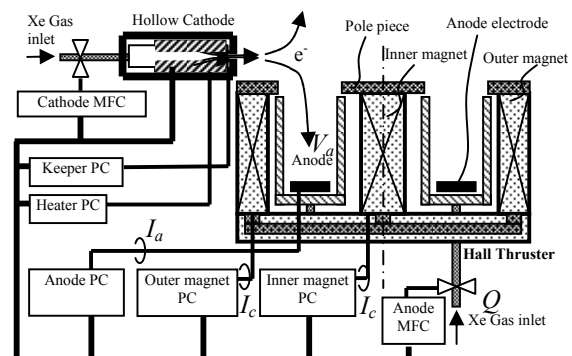


Fig. 1 Experimental setup: Hall thruster, power conditioners (PCs), and mass flow controllers (MFCs)

frequency analysis of the anode current waveform shown in Fig. 2. The oscillation frequencies measured in this study range from around 7 to 8 kHz.

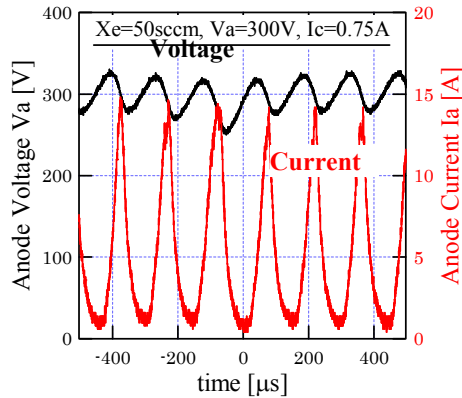


Fig. 2 Typical oscillating waveforms

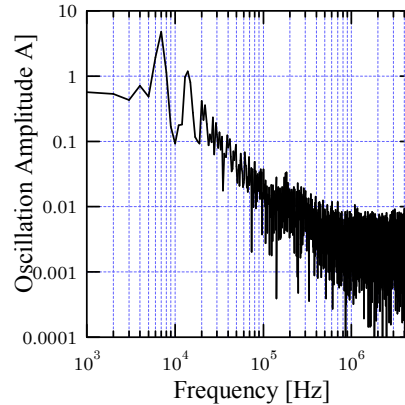


Fig. 3 Analysis of current waveform frequency shown in Fig. 2

In this study, we changed the external control parameters widely, that is,  $V_a$  from 200 to 325 V,  $Q$  from 50 to 150 sccm (standard cubic centimeters per minute), and  $I_c$  from 0.4 to 1.5 A (which corresponds to the magnetic flux density range of 10 to 29 mT at the channel exit), and measured the anode current waveform. Figure 4 shows the dependences of the measured oscillation strength on the anode voltage  $V_a$  and coil current  $I_c$  at a Xe flow rate of 50 sccm. The oscillation strength is not only sensitive to the coil current, that is, the magnetic flux density, but also depends on the anode voltage and gas flux. The oscillation strength  $\sigma$  is estimated as a standard deviation of  $I_a$  for discrete time measured by digital oscilloscope.

This measurement shows stable operating conditions. However, it shows simple and empirical sets of external control parameters. To develop an advanced and sophisticated control of Hall thrusters, such as an autonomous thruster, and to construct a physical model of the oscillation phenomenon, we must clarify some indicators of current oscillation, which are based on certain theoretical considerations.

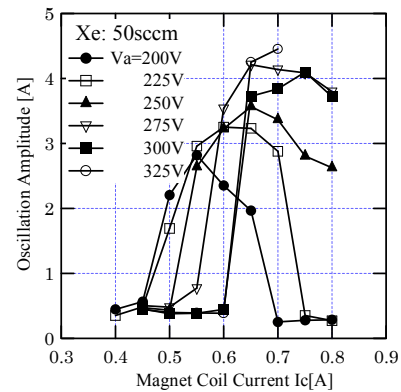


Fig. 4 Measured dependence of oscillation strength on anode voltage  $V_a$  and coil current  $I_c$  at Xe flow rate of 50 sccm

#### IV. Theory of Discharge Current Oscillation

The oscillation phenomenon of Hall thrusters depends on the magnetic flux density (coil current). It is generally considered that the anode current and oscillation strength of a Hall thruster depend on the magnetic flux density, as shown in Fig. 5 [8].

The mobility of electrons trapped by the magnetic field normally follows the mechanism of classical diffusion and is inversely proportional to the square of the magnetic flux density. However, when the magnetic flux density becomes larger than a certain threshold, the magnetic flux density dependence of mobility does not agree with the mechanism of classical diffusion; however, it agrees with the mechanism of anomalous diffusion, particularly Bohm

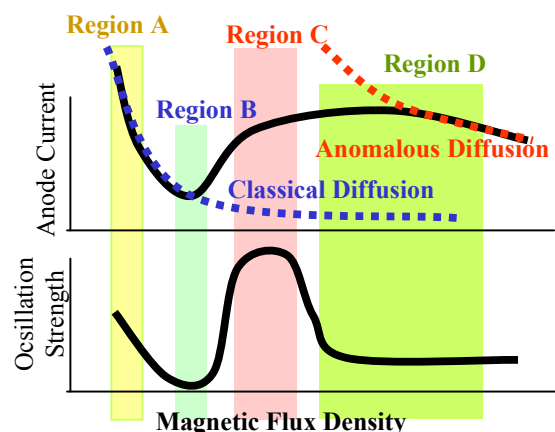


Fig. 5 Dependence of oscillation strength on magnetic flux density

diffusion [9]. In Bohm diffusion regions, the electron mobility is inversely proportional to the magnetic flux density.

Discharge current oscillation phenomena can be roughly classified into the four diffusion mode regions shown in Fig. 5. Region A is a weak-magnetic-flux-density region, where the confinement of electrons is insufficient and a relatively strong oscillation is observed. This region is not adequate for the ordinal operation of Hall thrusters. Region B is a classical diffusion region, where the oscillations are weak. It is desirable to operate in this region. Region C is a boundary region between the classical and anomalous diffusion regimes, where very severe oscillations are observed. This region must be avoided to achieve a stable operation. Region D is an anomalous diffusion region, where oscillations are relatively weak.

Many studies of the oscillation phenomena of Hall thrusters have been reported. Of these studies, the oscillation model presented by Yamamoto et al. [8] is very simple and suitable for the notional understanding of the oscillation phenomena. With reference to Ref. [8], we formulated a hypothesis in which the electron velocity has characteristic parameters for current oscillation.

The electron velocity is expressed as

$$V_e = \mu_e E + \frac{D}{N_e} \nabla N_e, \quad (1)$$

where  $\mu_e$  is the electron mobility,  $E$  is the electric field intensity,  $D$  is the diffusion constant, and  $N_e$  is the electron density number. In the classical diffusion region, the electron mobility can be expressed as

$$\mu_{e\_c} = \frac{mk_m}{qB^2} N_n, \quad (2)$$

where  $q$  is the electronic charge,  $B$  is the magnetic flux density,  $m$  is the electron mass, and  $k_m$  is the reaction rate coefficient of the momental transfer collision between electrons and neutral atoms.

In the Bohm diffusion region, it is expressed as [9]

$$\mu_{e\_a} = \frac{1}{16B}. \quad (3)$$

Assuming that the electric field intensity at the exit of the channel,  $E_x$ , is proportional to the anode voltage  $V_a$ , and the neutral gas density number  $N_{na}$  is proportional to the gas flux  $Q$ , and neglecting the diffusion term on the right side of Eq. (1), the electron velocity at the exit of the channel  $V_{ex}$  can be expressed proportionally as

$$V_{ex\_c} \cong \mu_{ex\_c} E_x \propto \frac{V_a \cdot Q}{B_x^2} \quad (4)$$

$$V_{ex\_a} \cong \mu_{ex\_a} E_x \propto \frac{V_a}{B_x} \quad (5)$$

Equation (4) shows the case of classical diffusion, and Eq. (5) shows the case of Bohm diffusion. The relation between the magnetic flux density  $B$  and the coil current  $I_c$  can be obtained by measurement. In particular, if  $B$  is smaller than the saturation magnetic flux density,  $B$  is proportional to  $I_c$ . From the above discussion, we hypothesized that the state of current oscillation can be simplified by the expressions shown in Eqs. (4) and (5).

## V. How to Determine Parameter Sets

For a comparatively weak magnetic flux density in the classical diffusion region, we measured the current waveform and its oscillation amplitude over wide anode voltage  $V_a$ , gas flux  $Q$  and coil current  $I_c$  ranges. Figure 6 shows a plot of the oscillation strength on the ordinate and the expression for classical diffusion (Eq. (4)) on the abscissa. In the same manner, Fig. 7 shows the oscillation strength and the expression for Bohm diffusion (Eq. (5)) for a comparatively strong magnetic flux density.

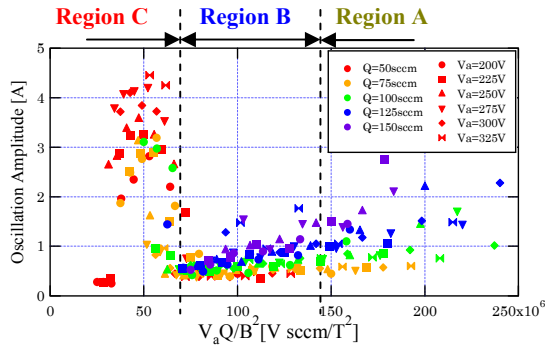


**Fig. 6** Oscillation amplitude of weak magnetic flux density region plotted versus expression in Eq. (4).

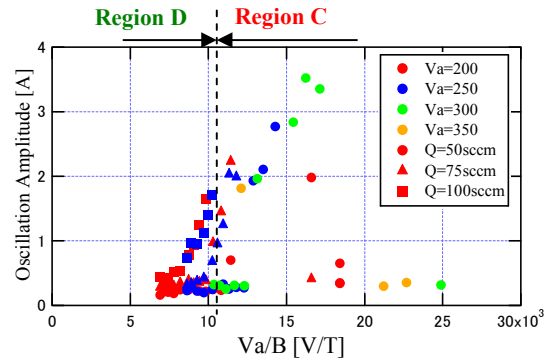


**Fig. 7** Oscillation amplitude of strong magnetic flux density region plotted versus expression in Eq. (5).

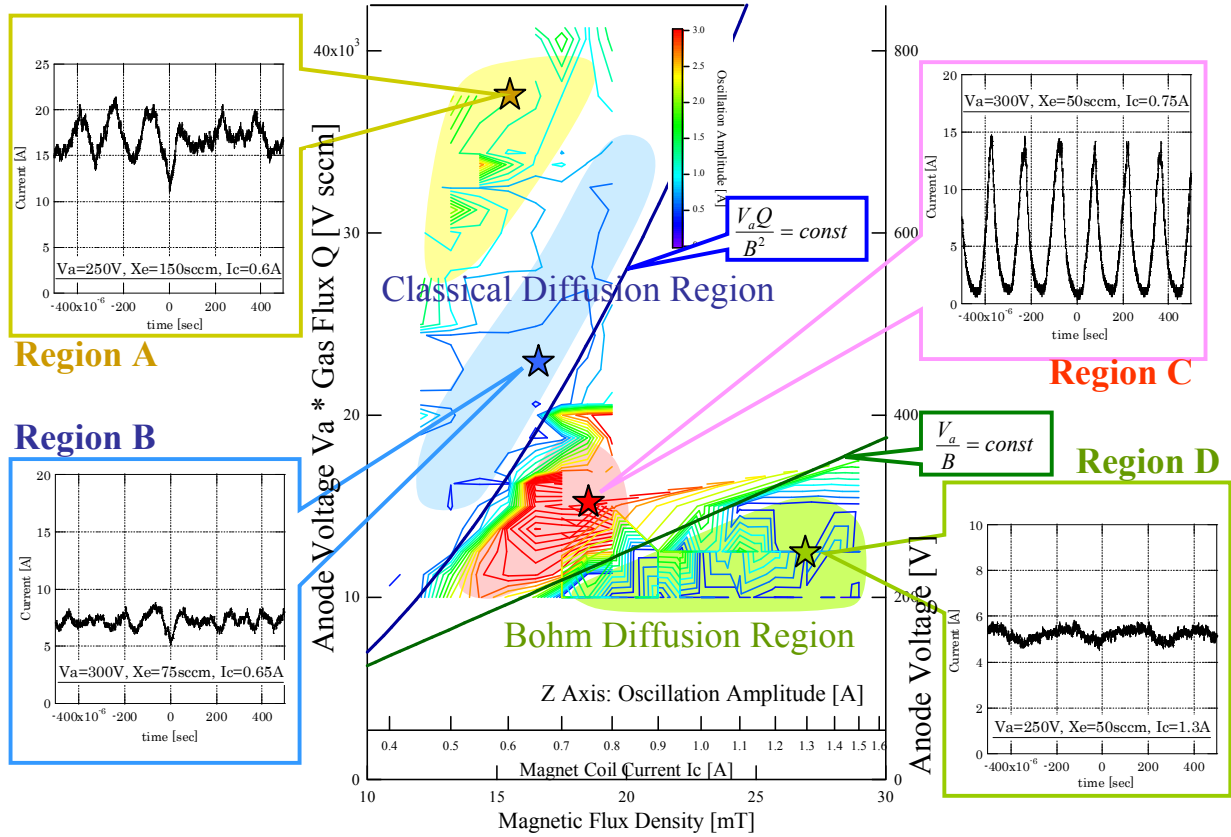


**Fig. 8** Operation conditions and oscillation mode regions

The 30<sup>th</sup> International Electric Propulsion Conference, Florence, Italy  
September 17-20, 2007

The oscillation strengths at various  $V_a$ ,  $Q$  and  $I_c$  values can systematically be arranged on the basis of the expressions Eqs. (4) and (5). As a result, we proved that our hypothesis is correct in that the state of current oscillation can be understood on the basis of the electron velocity, at least approximately. Simultaneously, we confirmed that the data measured at the weak (Fig. 6) and strong magnetic flux densities (Fig. 7) are for the regions of classical and Bohm diffusions, respectively.

By comparing these figures with Fig. 5, the four regions can be identified. In Fig. 6, the center of the two boundaries is Region B, where a stable operation is possible, and the left side is Region C, where a very strong oscillation may occur.

By applying this idea, Fig. 8 shows the contour plot of the oscillation amplitude. The left side of Fig. 8 shows the contour plot of Fig. 6, which is the classical diffusion region, and the oscillation amplitude contour is plotted with the product of the anode voltage  $V_a$  and gas flux  $Q$  on the ordinate, and the magnetic flux density (or coil current) on the abscissa. The right side of Fig. 7 shows the contour plot of the Bohm diffusion region, which is plotted with the anode voltage on the ordinate. The left and right sides of Fig. 8 are superimposed, fixing the gas flux  $Q$  at 50 sccm. (There is no significant reason for selecting this reference value.)

By making such a contour plot, one can observe very clearly how the oscillation mode changes with the magnetic flux density (coil current). The left region of classical diffusion and the right region of Bohm diffusion are combined through the boundary region C, and one can observe that the relative positions of the four regions can be located in one figure.

In Fig. 8, the bold line in the classical diffusion region is the line  $(V_a \times Q)/B^2 = const$ . Also, the bold line in the Bohm diffusion region is the line  $(V_a/B) = const$ , which corresponds to the dotted line in Fig. 7.

Typical current waveforms in each region are also shown in Fig. 8. In Regions C and D, the oscillating current waveforms are not simple sinusoidal waves, but have a characteristic shape. The shape and frequency of the waveforms have markedly changed between Regions C and D. By including such changes, Fig. 8 shows the oscillation mode of external control parameters.

## VI. Oscillation-free Operation by the Synchronous Control of Power Conditioners

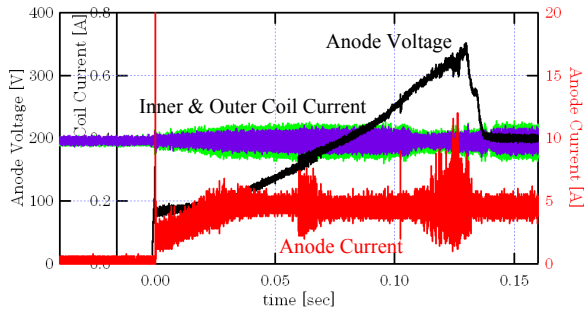
The oscillation suppression method is especially important when the operation or thruster conditions change temporally. When the operation conditions such as the anode voltage,  $V_a$ , or coil current,  $I_c$ , change transiently, the set of external control parameters may pass Region C, in which the current oscillation becomes very severe, and the momentary strong oscillation could have a fatal effect on the satellite system. If each power conditioner is synchronously controlled based on the oscillation mode regions shown in Fig. 8, an essentially oscillation-free operation can be realized even when the operation conditions such as  $V_a$  or  $I_c$  change transiently. In this section we discuss the case of power conditioner control at thruster start-up.

Figure 9 shows the voltage and currents waveforms of the conventional thruster start-up. Conventionally the coil currents are applied beforehand and kept constant, and then the anode voltage is applied. To prevent a rush current at the ignition, the anode voltage is applied slowly with a time constant of about 0.1 seconds. At the halfway through start-up, a current oscillation can be observed.

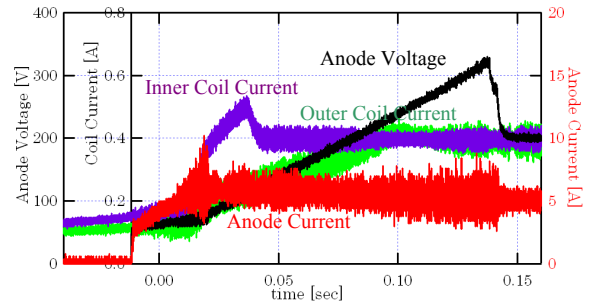
From Fig. 8, the boundary of Region B and Region C is the line  $(V_a \times Q)/B^2 = const$ . Because the gas flow rate  $Q$  can be considered as constant during the short start-up time, to pass through the stable region during the start-up the coil current should be controlled to roughly satisfy the relation  $V_a/B^2 = const$  according to the increase of the anode voltage.

Figure 10 shows the voltage and current waveforms when the coil current and anode voltage are synchronously controlled. The inner and outer coil currents began to flow a little before the anode voltage is applied, and the coil currents gradually increase according to the increase of the anode voltage.

Two improvements are obtained by this start-up method. One is that the current oscillation is suppressed at halfway through the voltage increase. Because both the anode voltage and coil currents synchronously increase, the set of parameters pass thorough only the stable operation region (Region B) and does not cross the boundary between Region B and Region C. The other improvement is that a pulse current does not occur at the moment of ignition. This is because the magnetic flux density is weak compared with the conventional start-up, and the ignition occurs at a comparatively small anode voltage.



**Fig. 9 Voltage and current waveforms of conventional start-up**



**Fig. 10 Voltage and current waveforms of start-up with synchronous control of PCs**

Figure 11 shows a trace of the magnetic flux density (coil currents) and anode voltage of the conventional (Fig. 9) and synchronous (Fig. 10) start-ups on the oscillation mode map shown in Fig. 8. Because the coil currents are kept constant, the conventional start-up crosses the boundary of Regions B and C. On the other hand, with the synchronous start-up, both the anode voltage and the coil currents are increased as the trace moves along the boundary, therefore essentially current oscillation does not occur. In this experiment, the target value of the anode voltage is 200 V, but we change the anode voltage from 0 V to over 300 V at start-up, which enable to observe the current oscillation over wide range of the anode voltage. In Fig. 11, the oscillation occurrence region is the boundary of the Regions B and C, and the Region A. As expected, the points of occurrence correspond to the passing of these oscillation occurrence regions. This result indicates that the current oscillation during anode voltage start-up can be thoroughly suppressed by controlling the power conditioners more accurately.

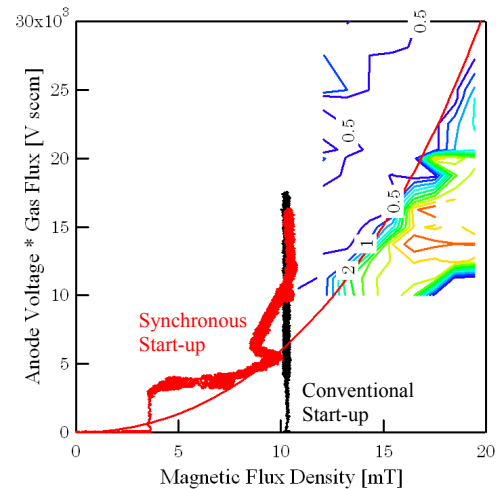


**Fig. 11 Trace of voltage and magnetic flux density on the oscillation mode map (Fig. 8)**

## VII. Considerations

In this study, we have successfully clarified the boundary of the oscillation and stable operation regions using the combination of external control parameters,  $(V_a \times Q/B^2)$  and  $(V_a/B)$ . Although the idea of using the expressions  $(V_a \times Q/B^2)$  and  $(V_a/B)$  is based on the theoretical considerations of electron velocity, it is not supported theoretically and can be considered an engineering approximation.

In this study, we assumed that the current oscillation depends only on three external control parameters, namely,  $V_a$ ,  $Q$  and  $I_c$ , which can be considered an ideal case. For practical applications, the other influences must be considered, such as temperature, channel wall abrasion and power supply characteristics, which are subject for future study.

Finally, we discuss the operating region and thruster performance. The ordinate in Fig. 8 shows the product of the anode voltage  $V_a$  and gas flux  $Q$ . By assuming that the gas flux is proportional to the anode current, the ordinate in Fig. 8 is roughly proportional to the electric power and thrust. When we fix the thrust and change the magnetic flux density, the oscillation strength decreases in Region B, in particular around the boundary of Regions B and C. On the other hand, the thrust efficiency does not maximize at the boundary of Regions B and C, and becomes slightly larger in the low magnetic-flux-density region. One of the reasons for this is that the electricity consumption of the magnets decreases. In addition, a low magnetic flux density requires small magnets, which is advantageous for weight reduction. Therefore, particularly in a large-thrust operation, it is better to choose a relatively low

magnetic flux density, that is, around the boundary of Regions B and A, as long as the discharge oscillation is allowable.

### VIII. Conclusion

We measured anode current oscillations over wide ranges of three external control parameters, namely,  $V_a$ ,  $Q$  and  $I_c$ . Then on the basis of the theoretical considerations of the oscillation phenomena, we analyzed the data on the basis of a hypothesis, that is, oscillation depends on the electron velocity. As a result, the oscillation mode can clearly be described using the expression  $(V_a \times Q/B^2)$  in the classical diffusion region and the expression  $(V_a/B)$  in the Bohm diffusion region. From these results, we successfully described an oscillation mode map, in which we can easily see the oscillation mode of all operation conditions.

And based on the oscillation mode map, controlling the anode voltage and coil currents synchronously, we show that the essentially oscillation free operation can be realized at the thruster start-up when the anode voltage changes transiently. The synchronous control of power conditioners is especially important when the operation conditions are transiently changes.

The expressions and the oscillation mode map provide very important guidelines for the stable control of Hall thrusters. For example, an autonomic operation will be possible for a Hall thruster system, including a power supply, to automatically determine the stable operation conditions for an externally given target thrust. Because the current oscillation can essentially be suppressed, it is possible to consider EMC measures for the other equipments in a satellite. Also, the optimization of the power supply design is possible, such as the reduction in power supply capacity. In the future, we believe that a sophisticated system management based on a physical model of the oscillation phenomena will be realized.

#### Acknowledgements

This work was performed under the Advanced Satellite Engineering Research Project contract sponsored by the Ministry of Economics, Trade and Industry (METI). We appreciate the advice and technical information provided by the following councilors of this project, Dr. H. Takegahara of Tokyo Metropolitan University, Dr. H. Kuninaka of the Japan Aerospace Exploration Agency, Dr. K. Komurasaki of the University of Tokyo, Dr. I. Kudou of Hokkaido University and Dr. H. Tahara of Osaka University. Also, we would like to acknowledge fruitful discussions with Dr. N. Yamamoto of Kyushu University.

#### References

- [1] T. Ozaki, Y. Inanaga, T. Nakagawa and H. Osuga, "DEVELOPMENT STATUS OF 200mN CLASS XENON HALL THRUSTER OF MELCO", IEPC-2005-064, November 2005.
- [2] H. Osuga, K. Suzuki, T. Nakagawa, T. Ozaki, I. Suga, T. Tamida, Y. Akuzawa, F. Soga, H. Suzuki, T. Furuichi and K. Matsui, "Development Status of Power Processing Unit for 250mN-class Hall Thruster", IEPC-2007-93 (*ibid.*).
- [3] E. Y. Choueiri, "Plasma oscillations in Hall thrusters", *Physics of Plasmas* Vol.8, No.4, 2001, pp.1411-1426
- [4] Baranov, V. I., Nazarenko, Yu. S., Petrosov, V. A., Vasin, A. I., and Yashnov, Yu. M., "Theory of Oscillation and Conductivity for Hall Thruster" AIAA-96-3192, 1996
- [5] Boeuf, J. P. and Garrigues, L., "Low frequency oscillation in a stationary plasma thruster" *J. Appl. Phys.*, Vol.84, No.7 (1998), pp.3541-3554
- [6] T. Tamida, T. Nakagawa, I. Suga, H. Osuga, T. Ozaki and K. Matsui, "Determining parameter sets for low-frequency-oscillation-free operation of Hall thruster" *J. Appl. Phys.*, Vol.102, 043304 (2007)
- [7] E. Y. Choueiri, "Fundamental difference between the two Hall thruster variants", *Physics of Plasmas* Vol.8, No.11, 2001, pp.5025-5033
- [8] N. Yamamoto, K. Komurasaki and Y. Arakawa, "Discharge Current Oscillation in Hall Thrusters", *J. Propul. Power*, Vol.21, No.5, pp.870-876 (2005)
- [9] Chambel, A.B., "Plasma Physics and Magnetofluidmechanics", McGraw-Hill, New York, 1963.